Measurements of angular distribution and spectrum of transition radiation with a GridPix detector

IOP Conf. Series: Journal of Physics: Conf. Series **934** (2017) 012049 doi:10.1088/1742-6596/934/1/012049

Measurements of angular distribution and spectrum of transition radiation with a GridPix detector

N Belyaev[1], M L Cherry[2], K Desch[3], K Filippov[1], P Fusco[4,5], J Kaminski[3], S Konovalov[6], D Krasnopevtsev[1], F Loparco[4,5], M N Mazziotta[5], D Ponomarenko[1], C Rembser[7], A Romaniouk[1], A Savchenko[1], E Shulga[1], S Smirnov[1], Yu Smirnov[1], V Sosnovtsev[1], P Spinelli[4,5], M Strikhanov[1], P Teterin[1], V Tikhomirov[1,6], K Vorobev[1] and K Zhukov[6]

[1] National Research Nuclear University MEPhI (Moscow Engineering Physics Institute), Kashirskoe highway 31, Moscow, 115409, Russia
[2] Dept. of Physics & Astronomy, Louisiana State University, Baton Rouge, LA 70803 USA
[3] University of Bonn, Germany
[4] Dipartimento di Fisica "M. Merlin" dell'Università e del Politecnico di Bari, I-70126 Bari, Italy
[5] Istituto Nazionale di Fisica Nucleare, Sezione di Bari, I-70126 Bari, Italy
[6] P. N. Lebedev Physical Institute of the Russian Academy of Sciences, Leninsky prospect 53, Moscow, 119991, Russia
[7] CERN, the European Organization for Nuclear Research, CH-1211 Geneva 23, Switzerland

E-mail: `Yury.Smirnov@cern.ch`

Abstract. In recent years, developments of gaseous detectors based on a combination of electron multiplication gap in the gas and pixel readout chips as a part of the anode plane (GasPixel detectors) reached a level where they can offer unique opportunities for particle detection. Transition radiation (TR) detectors based on this technology can be one of the possible applications. In this work, measurements of energy spectra and angular distributions of transition radiation photons produced by particles with different gamma factors made with a GridPix detector prototype are presented. The observed results are compared with theoretical predictions.

1. Introduction

GasPixel detector is one of the new promising technologies, which combines the properties of silicon and gaseous detectors. It has been extensively developed over the last decades (see review in [1] and also references in [2]). The operating principle of these detectors is similar to that of Time Projection Chambers with a two-dimensional readout plane. In this work the GasPixel detector with a special design called GridPix ([3]) was used. A schematic view of the GridPix detector is shown in figure 1. A specially treated pixel electronics chip (TimePix-1, [2, 4]) is placed in the gas volume. The gas volume has a drift gap (the width of the gap depends on the exact detector requirements) and an electron multiplication region. Electrons produced by an ionizing particle drift towards the pixel plane and develop an avalanche in the multiplication

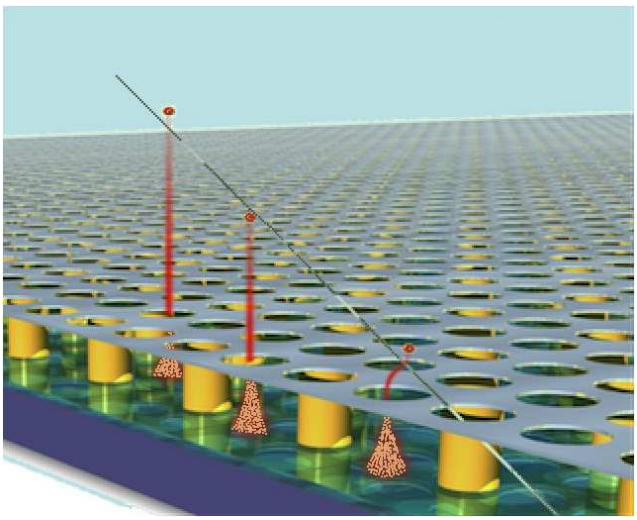

Figure 1. Schematic view of the GridPix detector (taken from [2]). The pixel chip is separated from a drift volume by a mesh. Electron amplification happens in the gap between the mesh and the pixel chip.

gap. The detectors are usually operated with an effective gas gain of $(2\text{–}5) \times 10^3$, which allows detection of single electrons with high efficiency. The chip has the possibility to choose an operation mode for each pixel: time or amplitude measurement. If time measurement mode is used, these detectors offer the possibility to reconstruct 3D track segments with a spacial accuracy of below 10 µm in a chip plane (see [1] and [2]). The GridPix detectors design (gas composition, drift gap, electronics) depends on the required functionality. Filled with Xe-based gas mixture, they may combine tracking and transition radiation detector properties (see [4]). In this case, the read-out electronics measures the signal amplitude in each pixel using Time-over-Threshold (ToT) information. The advantage of GridPix detectors as TRD devices is their capability to reconstruct a microscopic picture of ionization around a particle track and, hence, to maximize the separation between ionization and TR clusters. In a radiator medium, TR photons are generated at some angle to the particle direction, which depends on a particle's Lorentz factor. Using a GridPix detector, it is possible to identify photons not only by measuring ionization clusters along a track but also their distance from a track. This opens a possibility to improve particle identification properties of the detector. In this paper, spectra and angular distributions of TR photons measured by a GridPix detector are presented. They are compared with theoretical predictions.

2. Test beam setup

The experimental setup is shown schematically in figure 2. It contains a GridPix detector and TR radiator installed 2 meters upstream. In order to minimize TR photon absorption by air, a pipe filled with helium was placed between the radiator and the detector.

The GridPix test beam prototype was built on the basis of a Timepix chip (see details in [5]) with the pixel size of $55 \times 55\,\mu m^2$. The chip has a 256×256 pixel matrix providing $\approx 14 \times 14\,mm^2$ sensitive area. The detector is very similar to the one described in [6]. Only the cathode had been slightly modified and the readout electronics is based on the Scalable Readout System as described in [7]. The drift gap was chosen to be 3 cm and was filled with a mixture of Xe/CO_2 80%/20%. Electrical field in the drift gap was 900 V/cm. Charge deposited on each pixel was measured using Time-Over-Threshold method (ToT). A stack of 150 foils with a separation between foils of 2 mm was used as the TR radiator. Each radiator foil was made of 4 layers of polypropylene foils of 15.5 µm thick put on top of each other. The foils are held together by electrostatic forces without or with a very small (a few microns) air gap in between. Total thickness of such a radiator foil is about 62 µm. The tests were performed at the H8

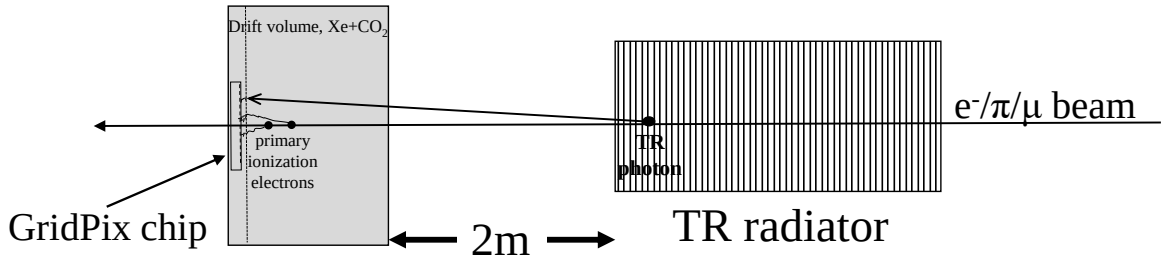

Figure 2. Schematic view of the experimental setup (not to scale).

SPS beam line at CERN with electrons and pions of 20 GeV ($\gamma = 3.9 \times 10^4$ and $\gamma = 1.4 \times 10^2$, respectively) and muons of 180 GeV ($\gamma = 1.7 \times 10^3$). The foils were oriented perpendicular to the beam and the detector plane had about 89° angle with respect to the beam line.

Figure 3 shows a typical event display with identified absorbed photons (black circles) and beam particle (red circle). Each point corresponds to one fired pixel and its color reflects

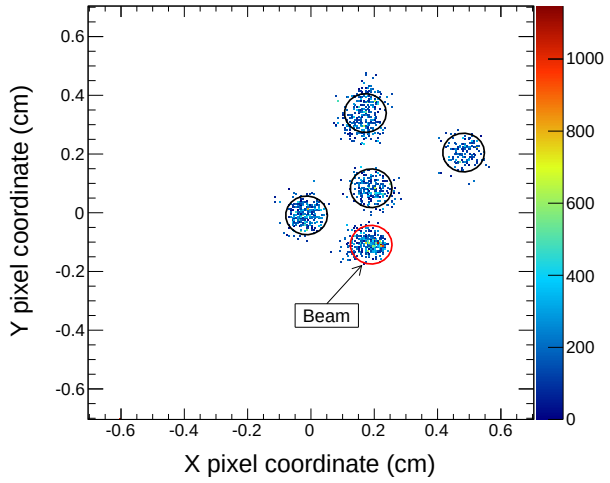

Figure 3. A typical event from the GridPix detector. Pixels fired by a beam particle are in the red circle.

the signal amplitude in this pixel. A group of adjacent fired pixels is referred to as a "cluster" throughout this paper, and it is an indication of a detected particle (beam particle, TR photon or a delta ray).

3. Results and discussion

In order to identify clusters in each event as shown in figure 3, a cluster search algorithm has been developed. It assumes that clusters have a circular shape. Besides being able to identify position of the clusters, the algorithm provides cluster geometry parameters and deposited energy calculated as a sum of ToT of all pixels within a circle. This allows separating clusters from beam particle and those originating from TR photons. In order to translate the sum of ToT of all pixels belonging to a cluster into an energy value, a calibration using 5.95 keV Fe^{55} source was performed. An energy resolution $\frac{\sigma_E}{E} = 14\%$ was obtained for this photon energy.

Photoelectrons from energetic photons have a significant pathlength in the gas and not all the energy can be accounted when a cluster is identified. In order to understand how this effect may affect the energy measurement, dedicated simulations based on the program developed in [8, 9] were performed. They include all processes occurring at photon absorption, photoelectron thermalisation, diffusion of secondary electrons drifting towards the anode plane. ToT is considered to be proportional to a number of electrons collected to one pixel.

Simulations show that, indeed, the average photoelectron path is significant and for photon energy of 10 keV it is ≈0.12 mm and for 20 keV it is ≈0.5 mm. Tails are extended up to several millimeters. Diffusion of secondary electrons drifting towards the anode also significantly contributes to the size of the ionization cluster seen by Pixel chip. The transverse diffusion coefficient of 176 $\mu m/\sqrt{cm}$ was initially calculated using the simulation package Garfield v.7.39 ([10]). But after comparison of the experimental data for Fe^{55} calibration run with the corresponding simulations the coefficient was corrected and the value of 210 $\mu m/\sqrt{cm}$ gave the best agreement of simulation with the data.

Distributions of ToT sum in identified clusters from absorbed photons with energy values of 10, 15 and 20 keV obtained in simulations are shown in figure 4. One sees that the higher is

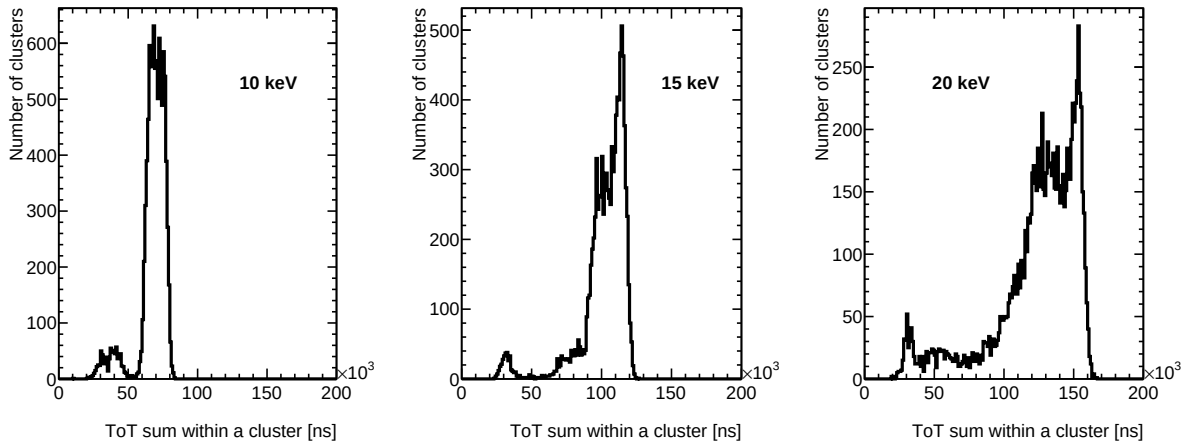

Figure 4. Simulated spectra of sums of pixels ToT for mono-energetic photons with energy values of 10 (a), 15 (b) and 20 keV (c). Simulation includes a detector response.

the photon energy, the wider is the distribution of measured ToT sum, because more pixels are not associated with the cluster. The initial simple algorithm for calculating the number of pixels in a cluster assumes its regular circular shape with a radius limited by 1.0 mm. Calculation of the cluster energy becomes less accurate as the cluster size grows and more pixels fall outside the assumed circular boundary. This unavoidably leads to a deformation of the measured TR spectrum in the energy range above ≈20 keV.

The measured distributions of the cluster multiplicity per event are shown in figure 5 for the case without radiator ((a), 20 GeV pions and electrons, 180 GeV muons) and with radiator ((b), 20 GeV electrons and 180 GeV muons).

Clusters not associated to the beam particle are referred to as "secondary" clusters in the text, whereas the other clusters are called the "primary" ones. In about 10% of events there are secondary clusters even without a radiator. They originate from delta-electrons and upstream bremsstrahlung photons (for electrons) absorbed in the detector. The number of events with

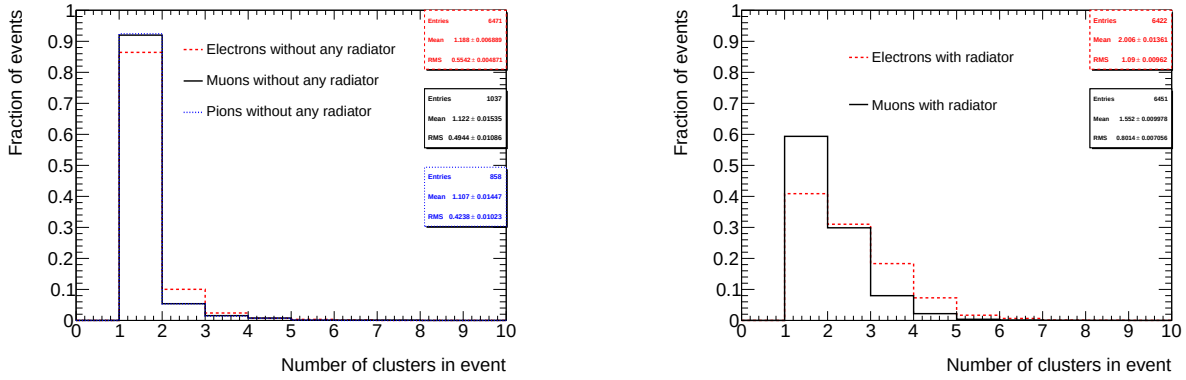

(a) (b)

Figure 5. Distributions of cluster multiplicity per event for different beam particles without (a) and with radiator (b).

clusters increases up to 60% for electrons and up to 40% for muons for the case with the radiator (plot (b) in figure 5). This corresponds to an average number of detected TR photons of 1.0 for electrons and 0.5 for muons. Not all of the clusters can be separated from the beam particle track. The typical size of a cluster is about 1 mm (see figure 3), which means that only clusters at least 1 mm apart from each other can be identified. This corresponds to an angle between a photon and a particle of about 0.5 mrad for the test beam geometry. A comparison of secondary cluster energy spectra for electrons of 20 GeV and 180 GeV muons is shown in figure 6 (a).

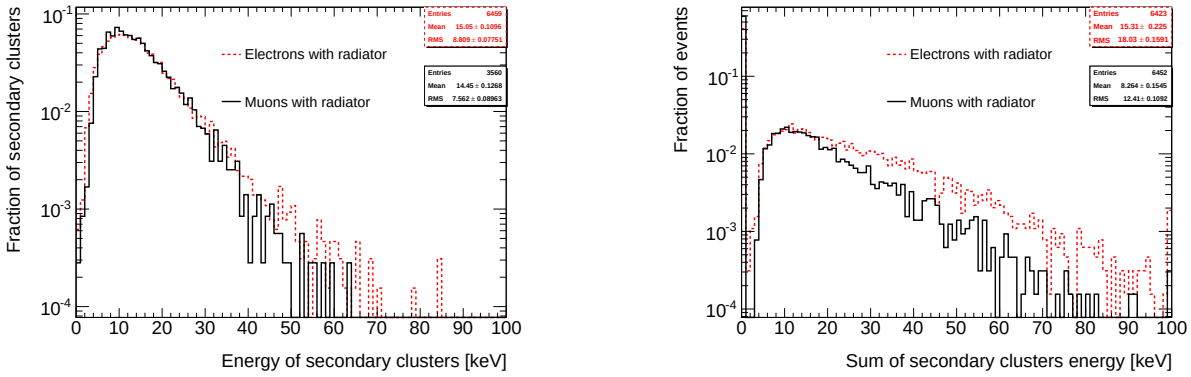

(a) (b)

Figure 6. (a): comparison of shapes of energy distributions of secondary clusters for electrons and muons. (b): distributions of sums of energies of secondary clusters in event for electrons and muons. Distributions are normalized to their own integrals. The rightmost bin on plot (b) includes overflown values.

The integral of each spectrum was normalized to 1 in this figure. One sees that in spite of the fact that the number of detected TR photons is almost two times less for muons, the shape of energy distribution is very close to that for electrons. The distributions of the sums of secondary clusters energies (total TR photons energy) per event are shown in figure 6 (b). These spectra are different because electrons produce more than one cluster more often.

The scatter plots of cluster energy vs. angle are presented in figure 7. Both distributions have the same number of beam particles.

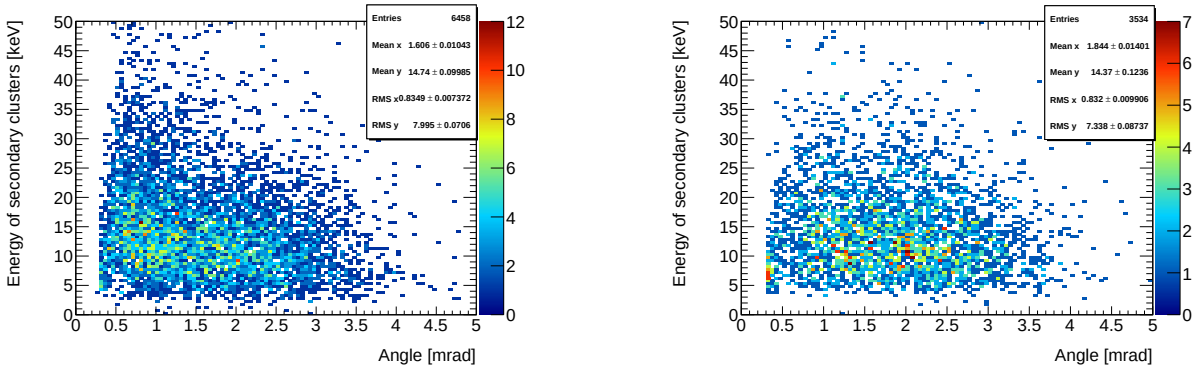

(a) (b)

Figure 7. Scatter plots of cluster energy vs. angle. Plot (a) is for electrons and plot (b) is for muons.

In general, the distributions look similar but one still observes some differences. In both cases TR is concentrated at angles below 4 mrad. Empty area below 0.3 mrad is defined by size of the cluster, which cannot be reconstructed too close to the primary particle cluster. This area increases with the photon energy because of a rise of the cluster size.

The projections of these distributions on the horizontal axis for the whole energy interval (a) and for energies below 15 keV (b) are shown in figure 8.

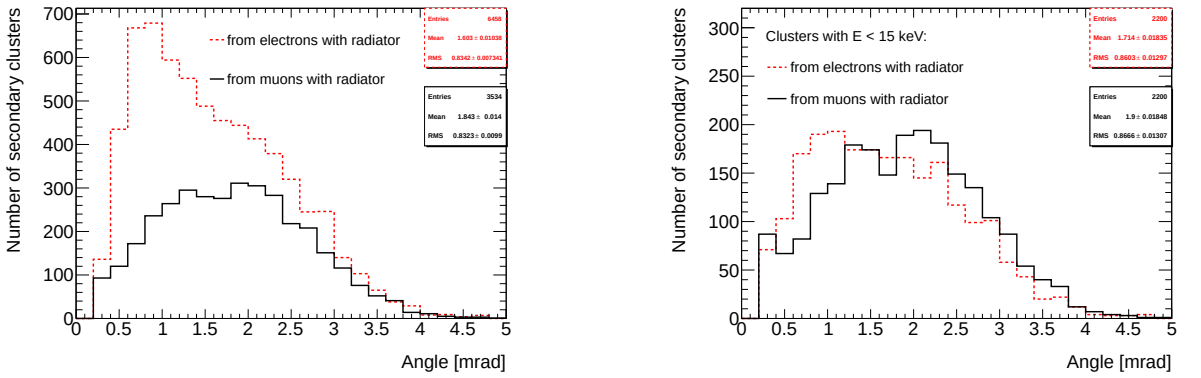

(a) (b)

Figure 8. Angular distribution of TR clusters for electrons and muons (plot (a) is for all energies, plot (b) is for energies below 15 keV).

TR photons originating from electrons have a tendency to concentrate at smaller angles. Some indication of a presence of two peaks in the muon distribution around 1 mrad and 2 mrad is also observed.

The TR is emitted along the particle at angles up to $\sqrt{\frac{1}{\gamma^2}+\frac{\omega_1^2}{\omega^2}}$, where $\omega_1 \approx 21$ eV is the plasma frequency of the CH_2 foils and ω is a TR photon energy. Angular distribution of photons at the last interference maximum is peaking up at the angle of $\sqrt{\frac{1}{\gamma^2}+\frac{\omega_2^2}{\omega^2}}$, where $\omega_2 \approx 0.7$ eV is the plasma frequency of air, which fills the space between the foils. For both 20 GeV electrons and 180 GeV muons one expects the maximum angle for TR photons in the energy range of 10–20 keV at ≈1 mrad. Less energetic photons should have wider distribution. In order to

understand the observed behavior in more details, a dedicated calculation based on exact TR production formulas ([11]) was performed. The calculations also include TR absorption in the radiator and in the detector materials.

The results of these calculations are shown in figure 9 (plot (a) for electrons and plot (b) is for muons).

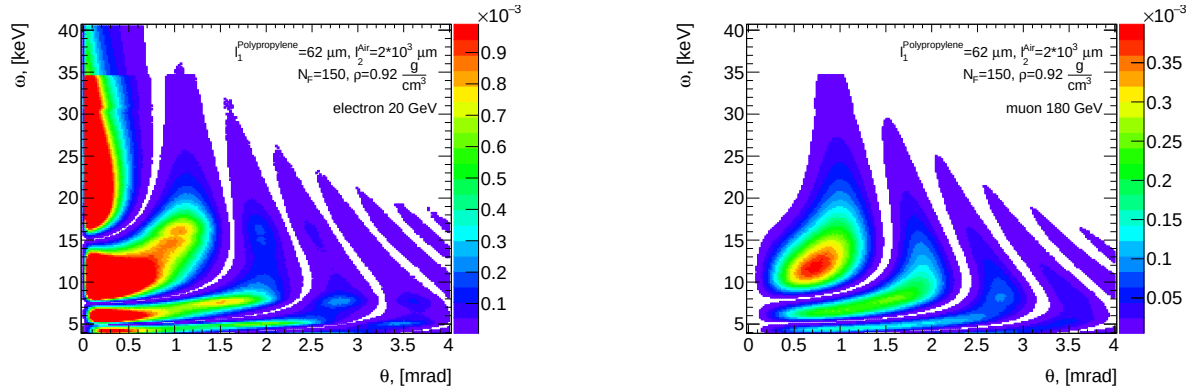

(a) (b)

Figure 9. Calculated scatter plots of cluster energy vs. angle: for electrons (a) and for muons (b).

One can clearly see that for electrons a significant part of TR is concentrated at angles below 0.5 mrad. As for the muons, only a small fraction of photons fall in this range. One also notices that the energy distribution of the TR clusters should have several peaks. The two most energetic ones are at ≈10 keV and ≈20 keV for electrons and ≈6 keV and ≈12 keV for muons. There is no significant difference between energy spectra observed in the data for these two sorts of particles. This can be explained by the fact that the most energetic photons produced by electrons are not reconstructed in the data because of minimal angle constraint. Limitations on the energy resolution for high energy photons also significantly deform spectrum. These two effects make measured spectra similar.

The projections of 2D distributions on horizontal axis are shown in figure 10.

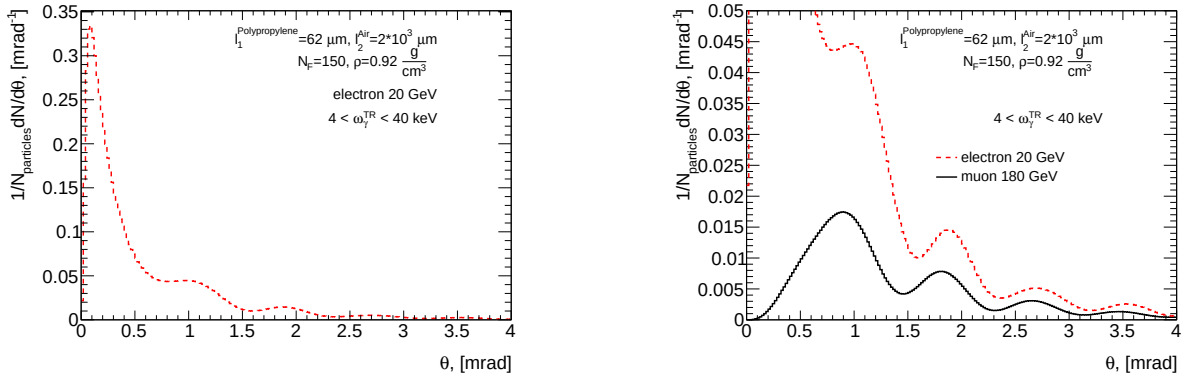

(a) (b)

Figure 10. Analytically calculated angular distributions of TR clusters for electrons (a) and for both electrons and muons (b).

Figure 10 (a) is for electrons and Figure 10 (b) is for muons and electrons. If we apply a requirement on a minimum reconstruction angle of 0.4 mrad, then about half of the TR photons are lost for electrons. The angular distributions for electrons and muons in the range above 0.5 mrad have quite a similar shape (plot (b) in figure 10), however, the number of TR photons is by about a factor of 2 smaller for muons, which is also observed in the data. The two strongest peaks in angular distributions in this range are clearly pronounced around 1 and 2 mrad. This is also seen in the data (see figure 8), however, the calculations predict a significantly stronger peak at ≈1 mrad than what is observed in the data.

4. Conclusions

Simultaneous measurement of angular and energy distributions of transition radiation photons were performed for the first time with the help of GridPix detector. No significant difference except in number of photons (by a factor of 1.8) between 20 GeV electrons ($\gamma = 3.9 \times 10^4$) and 180 GeV muons ($\gamma = 1.7 \times 10^3$) was observed. Angular distributions for electrons and muons are slightly different. Theoretical calculations of angular distributions predict a significantly different shape than the one observed in data. Calculations also predict a double-peak structure of the TR photons energy spectrum, which was not observed in data. The sources of all these discrepancies are the subject of future studies.

Acknowledgments

We gratefully acknowledge the financial support from Russian Science Foundation grant (project No. 16-12-10277).

References

[1] Olive K A *et al.* 2014 *Chin. Phys.* C **38** 090001
[2] Boldyrev A S *et al.* 2016 *Nucl. Instrum. Meth.* A **807** 47–55
[3] Kaminski J, Bilevych Y, Desch K, Krieger C and Lupberger M 2017 *Nucl. Instrum. Meth.* A **845** 233–5
[4] Hartjes F, Hessey N, Fransen M, Konovalov S, Koppert W, Morozov S, Romaniouk A, Tikhomirov V and Van der Graaf H 2013 *Nucl. Instrum. Meth.* A **706** 59–64
[5] Llopart X, Ballabriga R, Campbell M, Tlustos L and Wong W 2007 *Nucl. Instrum. Meth.* A **581** 485–94
[6] Krieger C, Kaminski J, Lupberger M and Desch K 2017 *Nucl. Instrum. Meth.* A **867** 101–7
[7] Lupberger M, Desch K and Kaminski J 2016 *Nucl. Instrum. Meth.* A **830** 75–81
[8] Azevedo C D R, Biagi S, Veenhof R, Correia P M, Silva A L M, Carramate L F N D and Veloso J F C A 2015 *Phys. Lett.* B **741** 272
[9] Biagi S 2017 Degrad URL `https://magboltz.web.cern.ch/magboltz/`
[10] Veenhof R 2010 Garfield – simulation of gaseous detectors URL `https://garfield.web.cern.ch/garfield`
[11] Cherry M L 1978 *Phys. Rev.* D **17** 2245